IEEE Access
Multidisciplinary : Rapid Review : Open Access Journal

Received May 17, 2021, accepted May 25, 2021, date of publication May 28, 2021, date of current version June 9, 2021.

Digital Object Identifier 10.1109/ACCESS.2021.3084823

SVM Aided Signal Detection in Generalized Spatial Modulation VLC System

HAOBO SUN[1], YANBIN ZHANG[1], FASONG WANG[1], JIANKANG ZHANG[1,2], (Senior Member, IEEE), AND SHIJIE SHI[1]

[1]School of Information Engineering, Zhengzhou University, Zhengzhou 450001, China
[2]Department of Computing and Informatics, Bournemouth University, Poole BH12 5BB, U.K.

Corresponding author: Yanbin Zhang (ieybzhang@zzu.edu.cn)

This work was supported in part by the National Natural Science Foundation of China under Grant 61571401, Grant U1736107, and Grant 61901366; in part by the National Natural Science Foundation of Henan Province under Grant 192102210088 and Grant 192102210091; in part by the Innovative Talent of Colleges and University of Henan Province under Grant 18HASTIT021; and in part by the National Key Research and Development Program under Grant 2019QY0302.

ABSTRACT Efficient signal detection technique is developed for generalized spatial modulation (GSM) modulated indoor visible light communication (VLC) system, which is aided by a popular machine learning approach termed as support vector machine (SVM). For general VLC system, maximum likelihood (ML) detector has a high computational complexity, although it is the optimal detection algorithm. In order to alleviate this high computational complexity problem, we take the signal detection task in GSM-VLC system as a multiple classification problem, and propose an efficient signal detection scheme for the considered GSM-VLC system aided by SVM, which has lower computational complexity and nearly optimal detection accuracy. Simulation results demonstrate the efficiency of the proposed SVM aided signal detection technique in the considered indoor GSM-VLC system.

INDEX TERMS Support vector machine (SVM), signal detection, visible light communication (VLC), generalized spatial modulation (GSM).

I. INTRODUCTION

In modern communication systems, radio frequency (RF) is the most widely used frequency band. However, due to the explosive growth of the Internet of Things and portable information terminals and the lack of spectrum resources, it is urgent to explore new spectrum to fundamentally solve the contradiction between the demand of super-capacity communication and the spectrum shortage. As an emerging technique of optical wireless communication (OWC), the visible light communication (VLC) system uses light emitting diodes (LEDs) as signal transmitter, which is capable of effectively solving the mentioned problems. It has been recognized as an effective supplement to RF communication by combining lighting and communication [1], [2]. In addition, VLC technology can also be applied to electromagnetic interference application scenarios where RF is not allowed or induces dangerous, such as hospitals, airplanes, mines, and many other areas [3], [4].

The associate editor coordinating the review of this manuscript and approving it for publication was Wei Feng.

At the physical layer transmission level, in view of the fact that multiple-input multiple-output (MIMO) transmission can deeply exploit wireless spatial resources, thereby significantly improving the system's spectrum efficiency, it has become one of research hotspots both in academia and industry. Generalized spatial modulation (GSM), as a new modulation technology in MIMO transmission technology [5], can effectively reduce the cost and complexity of the MIMO-VLC system in the actual application scenarios of the VLC system [6]–[8], wherein the transmitter uses the index information of the activated LEDs to carry information. Compared with traditional MIMO-VLC system, the GSM-VLC system can reduce the system complexity and obtain a higher spectrum efficiency [8]–[10].

As an emerging technology, so far, the main VLC research topic is focused on the structure of system transmission, while the research on performance analysis such as signal detection of the system is typically based on maximum likelihood (ML) optimal signal detection method [11]–[13]. However, the ML signal detector has the high computational complexity and it is not expandable along with the number of LEDs. Hence, how to reduce the complexity of signal detection under the premise of ensuring the signal detection performance of the system has become an important proposition to be solved.

In recent years, for the in-depth research in related fields of machine learning, it has been used to solve a series of engineering problems, especially in signal processing, pattern recognition, intelligent control and digital communication systems [14]. On signal detection in traditional RF wireless communication system, machine learning technology can effectively reduce the signal detection complexity while maintaining the bit error ratio (BER) performance of the system [15]–[17]. Specifically, a completely blind K-means clustering (KMC) detection algorithm for space shift keying (SSK) system was proposed in [15], however this detector has a certain error platform effect. Although it can be alleviated by increasing the number of algorithm executions, its complexity will increase greatly. In order to reduce the complexity of the algorithm, an improved K-means clustering (IKMC) detection algorithm was proposed in [16] by optimizing the initial clustering centers. However, the performance of the IKMC detector will deteriorate sharply as the cluster centers increase. Furthermore, a new blind detector termed as KMC based on the concept of constrained clustering was given in [17] by controlling the number of received symbols in each class, wherein the KMC detector's unconstrained optimization problem was converted into a constrained optimization problem, so as to obtain the optimized clustering centers to avoid system performance degradation caused by the increase in the number of clusters. The above methods mainly use unsupervised learning methods rather than supervised learning methods.

For VLC system, a signal detection method based on deep learning (DL) was proposed in [18], which integrated two connected multi-layer perception (MLP) networks into the receiving end and demodulated the received signal to complete the detection. Additionally, a DL-based auto-encoder for multi-dimensional color modulation of multi-color VLC system was considered in [19], which can effectively reduce the average symbol error ratio. Furthermore, for OFDM-VLC system, a signal detection algorithm based on support vector machine (SVM) was provided in [20]. However, none of the above methods consider applying machine learning technology to indoor MIMO GSM-VLC system.

In the indoor VLC system considered in this paper, due to the needs of lighting, multiple LED modules are generally arranged in the service space. Under this background, it is very suitable to use the GSM-VLC system to implement wireless communication services for application scenarios. Therefore, the indoor GSM-VLC system will be considered in this paper and the signal detection will be implemented by utilizing the SVM method in machine learning. Specifically, a training symbol data set is generated randomly and then a label vector of the training sample is constructed. Subsequently, the kernel SVM is used to construct the optimization problem of signal detection, and the convex dual problem of the original problem is obtained through transformation. As a result, the online signal detection for any given data stream is realized. In order to test the detection performance based on the SVM signal detection technology in the considered GSM-VLC system, the detection algorithm proposed was compared with multiple classical detection algorithms such as ML, KMC and IKMC through BER performance analysis. The simulation results show that the SVM aided detector can obtain better system detection performance in terms of the BER performance and the complexity.

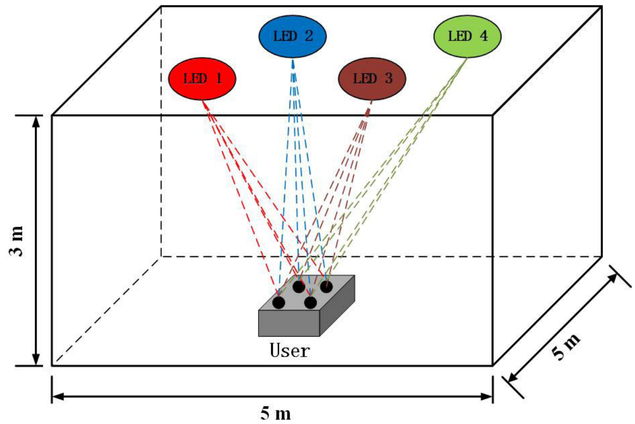

FIGURE 1. Conceptual diagram of indoor VLC system: $N_t = N_r = 4$, $\widetilde{L} = \widetilde{W} = 5$ m, $\widetilde{H} = 3$ m.

The following content of this paper is arranged as follows: The detailed mathematical model of the signal and VLC channel in the GSM-VLC system are described in Section II. In Section III, the SVM aided signal detection scheme and algorithm are presented in detail; The performance results and related discussions are provided in section IV. Finally, we provide our concluding remarks in Section V.

II. GSM-VLC SYSTEM AND SIGNAL MODELING

This paper considers an indoor GSM-VLC system based on intensity modulation (IM)/direct detection (DD) technology, where the transmitter uses multiple LEDs to send signals to the indoor randomly distributed user receivers. In this communication system, considering the indoor application environment of size $\widetilde{L} \times \widetilde{W} \times \widetilde{H}(\mathrm{m}^3)$, the transmitting end is equipped with N_t downward-mounted LEDs on the ceiling, and the receiving end is equipped with N_r upward photo-detectors (PDs) to communicate with the transmitting LEDs, as shown in Fig. 1. For simplicity, although not required, this paper assumes that all LEDs and PDs have the same parameters. In addition, it is further assumed that the transmitter can obtain the position of the receiver and channel state information (CSI) through some positioning methods of the VLC system. Therefore, the considered GSM-VLC system represents a typical MIMO-VLC Gaussian channel model.

The signal observed by the randomly distributed user receiving end PD is expressed as

$$\mathbf{y} = \mathbf{H}\mathbf{x} + \mathbf{w} \tag{1}$$

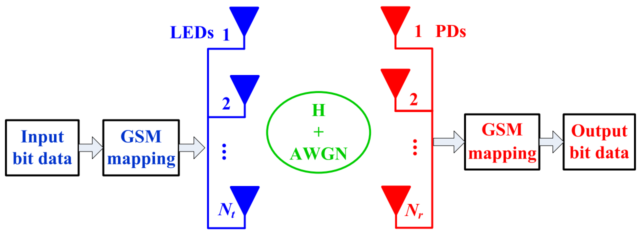

FIGURE 2. Block diagram of the considered GSM-VLC system.

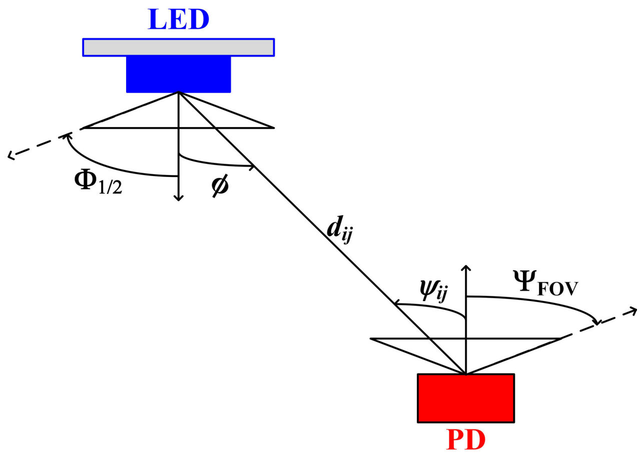

FIGURE 3. Schematic diagram of the geometric model of LoS transmission in VLC system.

where $\mathbf{H} \in \mathbb{R}_+^{N_r \times N_t}$ represents the channel gain between the transmitting end and the receiving end link, $\mathbf{x} = [x_1, x_2, \ldots, x_{N_t}]^{\mathsf{T}} \in \mathbb{R}^{N_t}$ represents the signal vector carrying information sent by the transmitter. In order to adjust the lighting level of the LED, it is assumed that the same direct current (DC) bias signal vector $\mathbf{I}_{\text{DC}} \in \mathbb{R}_+^{N_t}$ with identical element I_{DC} is superimposed on $\mathbf{x}$ in (1) [21]. In addition, in (1), $\mathbf{w} \sim \mathcal{N}(\mathbf{0}_{N_r}, \sigma^2 \mathbf{I}_{N_r})$ is the zero-mean additive white Gaussian noise (AWGN) received at the receiving end PD. The block diagram of GSM-VLC system is shown in Fig. 2.

In order to avoid clipping distortion, save power, and for safety, we can limit the total current $I_{\text{DC}} + x_i$ of the ith LED to the range of $[(1-\alpha)I_{\text{DC}}, (1+\alpha)I_{\text{DC}}]$, where $\alpha \in [0, 1]$ is called the modulation index [22]. At the same time, the information-carrying signal x_i must satisfy the peak amplitude constraint $|x_i| \leq A, \forall i$, where $A = \alpha I_{\text{DC}} \in \mathbb{R}_+$.

A. VLC CHANNEL MODEL

In indoor VLC, using the generalized Lambertian emission mode, the path gain G_{ij} between the jth LED and the ith PD can be expressed as [23]

$$G_{ij} = \begin{cases} \dfrac{1}{2\pi d_{ij}^2}(L+1)A_{\text{R}} \cos^L(\phi) \cos \psi_{ij}, & |\psi_{ij}| \leq \Psi_{\text{FoV}}, \\ 0, & |\psi_{ij}| > \Psi_{\text{FoV}} \end{cases} \tag{2}$$

where $\Phi_{1/2}$ is half irradiance angle, which is measured from the optical axis of the LED, and $L = -\ln(2)/\ln(\cos(\Phi_{1/2}))$ is the order of Lambertian emission. d_{ij} is the light-of-sight (LoS) distance between the jth LED and the ith PD. ϕ is the angle of irradiance of LED, ψ_{ij} is the angle of incidence of the jth LED and ith PD optical link, which is measured from the axis normal to the receiver surface. Also, for receiver, β is the refractive index of the optical concentrator and A_{PD} is the PD area. Finally, Ψ_{FoV} is the receiver's field-of-view (FoV) semi-angle. Then, the detection area of the PD is given by

$$A_{\text{R}} = \frac{\beta^2}{\sin^2(\Psi_{\text{FoV}})} A_{\text{PD}} \tag{3}$$

The geometric model of LoS transmission is demonstrated in Fig. 3. Please note that from (2) we can conclude that the path gain G_{ij} of the VLC system depends on the specific positions of the transmitter LED and the receiver PD. If the LED is not in the FoV at the receiving end, the link gain G_{ij} will be zero.

As a whole, the VLC channel gain between the jth LED and the ith PD of receiver can be expressed as

$$h_{ij} = TR\eta G_{ij}, \quad i = 1, 2, \ldots, N_r, \; j = 1, 2, \ldots, N_t \tag{4}$$

where T is the gain of the optical filter, R is the responsivity of the PD and η is the current-to-light conversion efficiency of the LEDs, respectively.

Additionally, for indoor VLC, the received light signals by the PDs of receiver are a summation of the LoS component and multiple non-LoS (NLoS) ones due to walls reflection of the service room. However, the total received optical power conveyed by the LoS link is more than 95% at the receiver. Moreover, even the strongest NLoS component is still at least 7 dB lower than the LoS one [23]. Consequently, when considering that the transmit LEDs are installed on the ceiling of the service area and face down-forwards, the channel model in Eq. (2) can neglect the NLoS components, but consider only the LoS component for carrying out tractable analysis. We note furthermore that the indoor VLC channel remains unchanged over thousands to millions of successive bits, and hence, it is considered quasi-static in the considered system [17].

B. SIGNAL MODEL

Let us assume that the transmitter is constituted by $\bar{N}$ LEDs in the considered service room. For our proposed GSM-VLC system, we assume that $N_t (N_t \leq \bar{N})$ LEDs are utilized for implementation of the GSM modulation among the $\bar{N}$ LEDs. During one specific symbol duration, among the selected N_t transmit LEDs, n_t LEDs are activated to transmit the specific information symbol, while the rest $(\bar{N} - n_t)$ LEDs are only used for illumination. Hence, there are in total $\bar{M} = \binom{N_t}{n_t}$ possible combinations, among which 2^{m_l} are used transmitting m_l bits per symbol, and $m_l = \lfloor \log_2 \binom{N_t}{n_t} \rfloor$, where $\lfloor . \rfloor$ denotes floor operation.

Furthermore, the length of the remaining bits per symbol is $m_s = \log_2(|\mathbb{M}|)$, where $|\mathbb{M}|$ is the order of the IM pulse amplitude modulation (PAM) constellation and is assumed to be the power of 2, and we further assume that $\mathcal{S} = \{s_m\}_{m=1}^{|\mathbb{M}|}$, where $s_m = \frac{2I_m}{|\mathbb{M}|+1}, m = 1, 2, \ldots, |\mathbb{M}|$, I is the mean optical intensity emitted. Therefore, the number of binary bits per GSM symbol is $n_{\text{GSM}} = m_l + n_t m_s = \lfloor \log_2 \bar{M} \rfloor + n_t \log_2(|\mathbb{M}|)$.

We assume that an independent and identically distributed (i.i.d.) random bit sequence $\{\ldots, b_1, b_2, \ldots, b_r, \ldots\}$ puts into the GSM mapper, where the bit sequence is divided into blocks of $n_{\text{GSM}} = \lfloor \log_2 \bar{M} \rfloor + n_t \log_2(|\mathbb{M}|)$ bits that are mapped into the GSM symbols $\mathbf{x}$, $\mathbf{x} \in \mathcal{X}$, and $\mathcal{X}$ is the $\binom{N_t}{n_t}|\mathbb{M}| = \bar{M}|\mathbb{M}|$ GSM symbols set. Aided by $\mathbf{x}$, special LEDs is selected to transmit a symbol with particular optical intensity chosen from the set of $\mathcal{S}$. Consequently, the selected LEDs will transmit the signal with a special intensity $s_m, m = 1, 2, \ldots, |\mathbb{M}|$ equiprobable at this particular time instant and all other LEDs remain silent just for lighting.

Hence, the transmitted GSM-VLC signal vector $\mathbf{x}$ can be expressed as follows

$$\mathbf{x} = [0 \ \ldots \ 0 \, s_{i_1} \, 0 \ \ldots \ 0 \, s_{i_2} \, 0 \ \ldots \ 0 \, s_{i_{n_t}} \, 0 \ \ldots \ 0]^{\mathrm{T}} + I_{\mathrm{DC}} 1 \, \mathbf{l} \tag{5}$$

where $i_j \in \{1, 2, \ldots, N_t\}, j = 1, 2, \ldots, n_t$, represents the index of the i_jth activated LED, $s_{i_1}, s_{i_2}, \ldots, s_{i_{n_t}} \in \mathcal{S}$, $\mathbb{1}$ denotes all-one column vector of length N_t. Accordingly, after removing the DC component I_{DC}, the received signals $\mathbf{y} \in \mathbb{R}^{N_r}$ could be simplified from (1) as

$$\begin{aligned} \mathbf{y} &= [\mathbf{h}_{i_1} \ldots \mathbf{h}_{i_{n_t}}][s_{i_1} \ldots s_{i_{n_t}}]^{\mathrm{T}} + \mathbf{w} \\ &= \sum_{\iota=i_1}^{i_{n_t}} \mathbf{h}_\iota s_\iota + \mathbf{w} = \mathbf{H}_\iota \mathbf{s} + \mathbf{w} \end{aligned} \tag{6}$$

where $\mathbf{H}_\iota = [\mathbf{h}_{i_1} \ \mathbf{h}_{i_2} \ \ldots \ \mathbf{h}_{i_{n_t}}]$ represents the submatrix of $\mathbf{H}$ with n_t columns, they are determined by the index of the n_tth activated LEDs, and $\mathbf{s} = [s_{i_1} \ s_{i_2} \ \ldots \ s_{i_{n_t}}]^{\mathrm{T}}$ denotes the transmit symbol vector corresponding to the LEDs $\iota = \{i_1, \ i_2, \ \ldots, i_{n_t}\}$.

Note that, the above described GSM-VLC system is reduced to the SM-VLC system, when $n_t = 1$. Intuitively, the SM-VLC scheme is a special case of our GSM-VLC, hence all the following results, conclusions, and detection algorithms that we describe for GSM-VLC system are easily transposed to the SM-VLC by letting $n_t = 1$.

III. SVM AIDED SIGNAL DETECTION OF GSM-VLC SYSTEM

A. CONVENTIONAL SIGNAL DETECTION BY MAXIMUM LIKELIHOOD

In our considered GSM-VLC systems, the task of the detector employed by receiver is to determine which data symbol and LEDs combination are selected by the transmitter during a symbol period, *i.e.*, to decide which channels are activated for delivering information, and the utilized data symbol intensity should also be decoded simultaneously. Since the LEDs combination and data symbol are equiprobably selected, the optimal detector employed by receiver can be designed by following the criterion of ML detection, which is expressed as

$$[\hat{i}_\iota, \hat{s}_m] = \underset{\iota \in \{1,\ldots,\bar{M}\}, s_m \in \mathcal{S}}{\arg\min} \|\mathbf{y} - \mathbf{H}_\iota \mathbf{s}\|_2^2 \tag{7}$$

where $\|\cdot\|_2$ denotes the Euclidean norm.

Then, the error performance of receiver employing the detector of (7) will be analyzed in detail. To begin with, the pairwise error probability of the detector at receiver is defined as the probability of detecting the symbol $\mathbf{s}_\nu$ transmitted from the $\bar{m}_\tau$th LEDs combination, while instead the $\bar{m}_\varsigma$th LEDs combination is actually activated and transmits symbol $\mathbf{s}_\mu$, which is denoted as $\mathrm{P}(\mathbf{H}_{\bar{m}_\varsigma}\mathbf{s}_\mu \mapsto \mathbf{H}_{\bar{m}_\tau}\mathbf{s}_\nu|\mathbf{H}, S)$ and can be expressed as

$$\begin{aligned} \mathrm{P}(\mathbf{k}_\mu^\varsigma \mapsto \mathbf{k}_\nu^\tau|\mathbf{H}, S) &= \mathrm{P}\left(\|\mathbf{y} - \mathbf{k}_\nu^\tau\|_2^2 > \|\mathbf{y} - \mathbf{k}_\mu^\varsigma\|_2^2\right) \\ &= \mathrm{P}\left(\|\mathbf{w}\|_2^2 > \|\mathbf{k}_\mu^\varsigma - \mathbf{k}_\nu^\tau - \mathbf{w}\|_2^2\right) \\ &= \mathrm{P}\left(2(\mathbf{k}_\mu^\varsigma - \mathbf{k}_\nu^\tau)^{\mathbf{T}}\mathbf{w} > \|\mathbf{k}_\mu^\varsigma - \mathbf{k}_\nu^\tau\|_2^2\right) \\ &= \mathcal{Q}\left(\frac{\|\mathbf{k}_\mu^\varsigma - \mathbf{k}_\nu^\tau\|}{2\sigma}\right) \end{aligned} \tag{8}$$

where $\mathbf{k}_\mu^\varsigma = \mathbf{H}_{\bar{m}_\varsigma}\mathbf{s}_\mu$ and $\mathbf{k}_\nu^\tau = \mathbf{H}_{\bar{m}_\tau}\mathbf{s}_\nu$, respectively. $\mathcal{Q}(\cdot)$ is the Gaussian Q-function, and is defined as $\mathcal{Q}(x) = \frac{1}{\sqrt{2\pi}} \int_x^\infty \exp\left\{-\frac{t^2}{2}\right\} dt$.

Consequently, with the aid of the union-bound approach [24], we can express the upper-bound BER at receiver as

$$\begin{aligned} \mathrm{P}_{\text{bit}} \leq & \frac{1}{n_{\text{GSM}}|\mathcal{X}|} \sum_{\bar{m}_\varsigma=1}^{\bar{M}} \sum_{\mu=1}^{|\mathbb{M}|} \sum_{\bar{m}_\tau=1}^{\bar{M}} \sum_{\nu=1}^{|\mathbb{M}|} H_d\left(\mathbf{H}_{\bar{m}_\varsigma}\mathbf{s}_\mu \mapsto \mathbf{H}_{\bar{m}_\tau}\mathbf{s}_\nu\right) \\ & \times \mathrm{P}(\mathbf{H}_{\bar{m}_\varsigma}\mathbf{s}_\mu \mapsto \mathbf{H}_{\bar{m}_\tau}\mathbf{s}_\nu|\mathbf{H}, S) \\ = & \frac{1}{n_{\text{GSM}}|\mathcal{X}|} \sum_{\bar{m}_\varsigma=1}^{\bar{M}} \sum_{\mu=1}^{|\mathbb{M}|} \sum_{\bar{m}_\tau=1}^{\bar{M}} \sum_{\nu=1}^{|\mathbb{M}|} H_d\left(\mathbf{H}_{\bar{m}_\varsigma}\mathbf{s}_\mu \mapsto \mathbf{H}_{\bar{m}_\tau}\mathbf{s}_\nu\right) \\ & \times \mathcal{Q}\left(\frac{\|\mathbf{k}_\mu^\varsigma - \mathbf{k}_\nu^\tau\|}{2\sigma}\right) \end{aligned} \tag{9}$$

where $H_d\left(\mathbf{H}_{\bar{m}_\varsigma}\mathbf{s}_\mu \mapsto \mathbf{H}_{\bar{m}_\tau}\mathbf{s}_\nu\right)$ is the Hamming distance between the bits representations of $\mathbf{H}_{\bar{m}_\varsigma}\mathbf{s}_\mu$ and $\mathbf{H}_{\bar{m}_\tau}\mathbf{s}_\nu$.

B. CONCEPT OF SVM

SVM is a classical supervised classification method in machine learning society, which has been widely used in signal processing, pattern recognition, image analysis and digital communication systems [10]. In fact, the classical SVM is a two-class classifier, which classifies the convex hulls of two disjoint samples in the space by generating a hyperplane to find the maximum margin. The subset of samples closest to the hyperplane is termed as support vectors, which can be utilized to determine the location of the separating hyperplane. For the linearly separable problem in an n-dimensional feature space with feature vector $\mathbf{v}$, the hyperplane can be described as

$$G(\mathbf{v}) = \mathbf{w}^{\mathbf{T}}\mathbf{v} + \varrho = 0 \tag{10}$$

where $\mathbf{w}$ is the normal vector, which determines the direction of the hyperplane, ϱ is a scalar constant that controls the distance between the hyperplane and the origin. Obviously, the hyperplane can be determined by the normal vector $\mathbf{w}$ and the displacement term ϱ. The hyperplane $G(\mathbf{v})$ is learned using P elements training data set $\{\mathbf{v}_p, u_p\}, p = 1, \ldots, P$ and $P = P^+ + P^-$, where $\mathbf{v}_p \in \mathbb{R}^n$ is feature vector, $u_p \in \{+1, -1\}$ is the label, P^+ and P^- represent the numbers belonging to labels $+1$ and -1, respectively.

In order to maximize the distance between the hyperplane and the training samples that are closest to the considered hyperplane, the parameters $\mathbf{w}$ and ϱ can be readjusted to make these points lie on either hyperplane $\{\mathbf{v} \mid \mathbf{w}^{\mathsf{T}}\mathbf{v} + \varrho = -1\}$ or $\{\mathbf{v} \mid \mathbf{w}^{\mathsf{T}}\mathbf{v} + \varrho = +1\}$. Consequently, the distance between these two parallel hyperplane is termed as margin and equals $\frac{2}{\|\mathbf{w}\|_2^2}$, where $\|\cdot\|_2$ is used to denote the Euclidean norm. Then, by introducing the sign variables u_p and simple operations, the classification problem is turned to a convex optimization problem, which can be expressed as

$$\begin{aligned} &\min_{\mathbf{w},\varrho} \ \frac{1}{2}\|\mathbf{w}\|_2^2 \\ &\text{s.t. } u_p(\mathbf{w}^{\mathsf{T}}\mathbf{v}_p + \varrho) \geq 1, \quad p = 1, \ldots, P \end{aligned} \tag{11}$$

The optimization problem of (11) is a convex quadratic programming problem, it could be resolved by existing software package. Actually, the problem of (11) can also be solved by its Lagrange dual problem more efficiently by lagrangian multiplier method, the corresponding generalized Lagrangian function of optimization problem (11) can be written as

$$L(\mathbf{w}, \varrho, \boldsymbol{\alpha}) = \frac{1}{2}\|\mathbf{w}\|_2^2 - \sum_{p=1}^{P} \alpha_p[(\mathbf{w}^{\mathsf{T}}\mathbf{v}_p + \varrho) - 1] \tag{12}$$

where $\boldsymbol{\alpha} = [\alpha_1, \ldots, \alpha_P]^{\mathsf{T}} \in \mathbb{R}_+^P$ is the associated Lagrange multiplier vector or termed as dual variable vector. Due to the Karush-Kuhn-Tucker conditions for differentiable convex problem, we can arrive at the dual problem of the optimization problem (11) as

$$\begin{aligned} &\max_{\boldsymbol{\alpha}} \ \sum_{p=1}^{P} \alpha_p - \frac{1}{2}\sum_{p=1}^{P}\sum_{q=1}^{P} u_p u_q \alpha_p \alpha_q \mathbf{v}_p^{\mathsf{T}}\mathbf{v}_q \\ &\text{s.t. } \sum_{p=1}^{P} u_p \alpha_p = 0, \\ &\quad \alpha_p \geq 0, \quad p = 1, \ldots, P \end{aligned} \tag{13}$$

Suppose the optimal solution of the primal and dual optimization problem in (11) and (13) are denoted as $\mathbf{w}^\star, \varrho^\star, \boldsymbol{\alpha}^\star$, respectively. Then, the parameters $\mathbf{w}^\star$ and $\varrho^\star$ can be represented by $\boldsymbol{\alpha}^\star$ respectively as

$$\mathbf{w}^\star = \sum_{p=1}^{P} \alpha_p^\star u_p \mathbf{v}_p \tag{14}$$

$$\varrho^\star = \frac{1}{|\mathcal{V}|}\sum_{n\in\mathcal{V}} \left[u_n - \mathbf{w}^{\star\mathsf{T}}\mathbf{v}_n\right] \tag{15}$$

where $\mathcal{V}$ is the index set of all support vectors and $|\mathcal{V}|$ denotes the cardinality of set $\mathcal{V}$. Hence, for any new coming feature vector $\mathbf{v}$, the decision of classification can be obtained by

$$\text{sign}\left[\mathbf{w}^{\star\mathsf{T}}\mathbf{v} + \varrho^\star\right] = \text{sign}\left(\sum_{p=1}^{P} \alpha_p^\star u_p \mathbf{v}_p^{\mathsf{T}}\mathbf{v} + \varrho^\star\right) \tag{16}$$

Nevertheless, for general classification problem, the training data samples cannot be separate by a hyperplane. In this case, the kernel SVM is proposed by using a nonlinear classification function $\tilde{G}(\mathbf{v}) = \mathbf{w}^{\mathsf{T}}\phi(\mathbf{v}) + \varrho$, similarly with (11), we have the following convex quadratic programming problem

$$\begin{aligned} &\min_{\mathbf{w},\varrho} \ \frac{1}{2}\|\mathbf{w}\|_2^2 \\ &\text{s.t. } u_p(\mathbf{w}^{\mathsf{T}}\phi(\mathbf{v}_p) + \varrho) \geq 1, \quad p = 1, \ldots, P \end{aligned} \tag{17}$$

Then the dual problem of (17) can be expressed as

$$\begin{aligned} &\max_{\boldsymbol{\alpha}} \ \sum_{p=1}^{P} \alpha_p - \frac{1}{2}\sum_{p=1}^{P}\sum_{q=1}^{P} u_p u_q \alpha_p \alpha_q (\phi(\mathbf{v}_p))^{\mathsf{T}}\phi(\mathbf{v}_q) \\ &\text{s.t. } \sum_{p=1}^{P} u_p \alpha_p = 0, \\ &\quad \alpha_p \geq 0, \quad p = 1, \ldots, P \end{aligned} \tag{18}$$

By defining the kernel function $\kappa(\mathbf{a}, \mathbf{b}) = (\phi(\mathbf{a}))^{\mathsf{T}}\phi(\mathbf{b})$, (18) can be expressed as

$$\begin{aligned} &\max_{\boldsymbol{\alpha}} \ \sum_{p=1}^{P} \alpha_p - \frac{1}{2}\sum_{p=1}^{P}\sum_{q=1}^{P} u_p u_q \alpha_p \alpha_q \kappa(\mathbf{v}_p, \mathbf{v}_q) \\ &\text{s.t. } \sum_{p=1}^{P} u_p \alpha_p = 0, \\ &\quad \alpha_p \geq 0, \quad p = 1, \ldots, P \end{aligned} \tag{19}$$

For real Euclidean space, the kernel function $\kappa(\cdot, \cdot)$ can be chosen arbitrarily by the guarantee by Mercer's condition. There are several popular kernel function in practice, which are listed as follows

$$\begin{aligned} &\textit{Linear Kernel}: \kappa(\mathbf{a}_1, \mathbf{a}_2) = \mathbf{a}_1^{\mathsf{T}}\mathbf{a}_2 \\ &\textit{Gaussian Kernel}: \kappa(\mathbf{a}_1, \mathbf{a}_2) = \exp\left(-\frac{\|\mathbf{a}_1 - \mathbf{a}_2\|_2^2}{2\sigma^2}\right) \\ &\textit{Laplace Kernel}: \kappa(\mathbf{a}_1, \mathbf{a}_2) = \exp\left(-\frac{\|\mathbf{a}_1 - \mathbf{a}_2\|_2}{\sigma}\right) \\ &\textit{Sigmoid Kernel}: \kappa(\mathbf{a}_1, \mathbf{a}_2) = \tanh\left(\beta\mathbf{a}_1^{\mathsf{T}}\mathbf{a}_2 + \theta\right) \end{aligned} \tag{20}$$

Suppose the optimal solution of the primal and dual optimization problem in (17) and (18) are denoted as $\mathbf{w}^\star, \varrho^\star, \boldsymbol{\alpha}^\star$, respectively. Then, the parameters $\mathbf{w}^\star$ and $\varrho^\star$ can be represented by $\boldsymbol{\alpha}^\star$ respectively as

$$\mathbf{w}^\star = \sum_{p=1}^{P} \alpha_p^\star u_p \phi(\mathbf{v}_p) \tag{21}$$

$$\varrho^\star = \frac{1}{|\mathcal{V}|}\sum_{n\in\mathcal{V}} \left[u_n - \mathbf{w}^{\star\mathsf{T}}\phi(\mathbf{v}_n)\right] \tag{22}$$

TABLE 1. An example GSM mapping table with $N_t = 5, n_t = 2, M = 2$.

Bits	Symbol bits	Symbols	Spatial bits	LED index	Label
0000	0	$\frac{2}{3}$	000	1 & 2	1
0001	1	$\frac{4}{3}$	000	1 & 2	2
0010	0	$\frac{2}{3}$	001	1 & 3	3
0011	1	$\frac{4}{3}$	001	1 & 3	4
0100	0	$\frac{2}{3}$	010	1 & 4	5
0101	1	$\frac{4}{3}$	010	1 & 4	6
0110	0	$\frac{2}{3}$	011	1 & 5	7
0111	1	$\frac{4}{3}$	011	1 & 5	8
1000	0	$\frac{2}{3}$	100	2 & 3	9
1001	1	$\frac{4}{3}$	100	2 & 3	10
1010	0	$\frac{2}{3}$	101	2 & 4	11
1011	1	$\frac{4}{3}$	101	2 & 4	12
1100	0	$\frac{2}{3}$	110	2 & 5	13
1101	1	$\frac{4}{3}$	110	2 & 5	14
1110	0	$\frac{2}{3}$	111	3 & 4	15
1111	1	$\frac{4}{3}$	111	3 & 4	16

where $\mathcal{V}$ is the index set of all support vectors and $|\mathcal{V}|$ denotes the cardinality of set $\mathcal{V}$. Hence, for any new coming data $\tilde{\mathbf{v}}$, the decision of classification can be obtained by (16).

C. SIGNAL DETECTION SCHEME AIDED BY SVM

In this subsection, an SVM aided signal detection algorithm is proposed with low complexity and good performance of the considered GSM-VLC system. Speifically, by using the classification idea of SVM, a four-stage signal detection strategy is proposed, which is termed as: 1) Generating training data set; 2) Labeling samples; 3) Building learning system; 4) Signal detection. The detailed procedures are elaborated on as follows.

1) GENERATING TRAINING DATA SET

Generally, the training data set is the input of the SVM learning system, which is constituted by part of the received signal $\mathbf{y}$. In our considered GSM-VLC system, the transmitted data bits at any particular time instant consist of two groups, the first group contains $\lfloor \log_2 \binom{N_t}{n_t} \rfloor$ bits and activates LEDs combination selected from the set of N_t LEDs, where n_t is the number of LEDs activated simultaneously in each time instant, the second group with $\log_2 |\mathbb{M}|$ bits modulates a signal constellation symbol from the PAM. Assuming that the number of transmitting LEDs is N_t and the number of signal constellation symbols is $|\mathbb{M}|$, then in our GSM-VLC system, $\eta_{\text{GSM}} = \lfloor \log_2 \binom{N_t}{n_t} \rfloor + \log_2 |\mathbb{M}|$ data bits can be transmitted at any time instants. As an example and without loss of generality, assuming that $N_t = 5$, $n_t = 2$ and $M = 2$, *i.e.*, the number of intensity levels is 2 and $I_1 = \frac{2}{3}$, $I_2 = \frac{4}{3}$, in this special GSM-VLC system, the mapping table is illustrated in Table 1.

Based on this mapping rule, the transmitted signal $\mathbf{x}$ can be obtained according to the described mapping criteria. Then, by performing the following steps, the training samples $\mathbf{y}$ can be obtained.

- Step 1: The signal vector to be transmitted $\mathbf{x} = [x_1, x_2, \ldots, x_{N_t}]^{\mathsf{T}} \in \mathbb{R}^{N_t}$ is generated from the mapping criteria.
- Step 2: Passing the generated transmission signal through the channel $\mathbf{H} \in \mathbb{R}_+^{N_r \times N_t}$ of the VLC system corrupted by AWGN.
- Step 3: Generating the received signal vector $\mathbf{y}$ according to Eq. (1), and taking part of $\mathbf{y}$ as the training data set.

2) LABELING SAMPLES

From Table 1, we will learn that the LEDs combination index and symbols can be identified effortlessly, and hence we can label the transmitted signals according to the LEDs combination index and symbols aided by mapping criteria. Suppose that the combination of the label set and a collection of bit information are denoted by $\mathbb{L}$ and $\mathbb{I}$, respectively. As discussed, there exists a one-to-one mapping between $\mathbb{L}$ and $\mathbb{I}$. A quintessential example should be cited that labels for a special GSM-VLC system are demonstrated in Table 1, where $N_t = 5$, $n_t = 2$ and $M = 2$. The detailed labeling procedure can be summarized as the following steps.

- Step 4: Generating $\eta_{\text{GSM}} P$ bits stream $\mathbb{I}$ randomly, then every successive η_{GSM} bits are taken as a group. As a result, we obtain P data bits groups.
- Step 5: According to the mapping criteria proposed above, for the pth bits group $i_p \in \mathbb{I}$, we can obtain the corresponding label $l_p \in \mathbb{L}$.
- Step 6: Repeating Step 5 until the corresponding labels of all samples $i_p, p = 1, 2, \ldots, P$ are obtained, thus forming the label vector $\mathbf{b}$.

3) BUILDING LEARNING SYSTEM

Through the above arranged steps, using the obtained received signal $\mathbf{y}$ and its corresponding label vector $\mathbf{b}$, a learning system for multiple classifications can be constructed to complete the classification and detection of the received signal. The detailed process is as follows:

- Step 7: Normalizing the data set.
- Step 8: One-vs-rest ($l - \text{vs} - \bar{l}$) binary label classification method: As stated before, for general classification problem, training feature samples are generally unseparable by a single hyperplane linearly. In order to commence this problem, the kernel SVM is used to obtain the following convex quadratic optimization problem aided by slack variables and KKT conditions

$$\begin{aligned} \max_{\boldsymbol{\alpha}} \quad & \sum_{p=1}^{P} \alpha_p - \frac{1}{2} \sum_{p=1}^{P} \sum_{\tilde{p}=1}^{P} b_{l_p} b_{l_{\tilde{p}}} \alpha_p \alpha_{\tilde{p}} \kappa(\mathbf{d}_p, \mathbf{d}_{\tilde{p}}) \\ \text{s.t.} \quad & \sum_{p=1}^{P} \alpha_p b_{l_p} = 0, \\ & 0 \le \alpha_p \le \tilde{C}, \quad p = 1, \ldots, P \end{aligned} \tag{23}$$

where $\tilde{C} \in \mathbb{R}_+$ is the penalty coefficient, which is employed to balance the model bias and over fitting, $\boldsymbol{\alpha} \in \mathbb{R}_+^P$ is the dual variable vector. $\kappa(\mathbf{d}_p, \mathbf{d}_{\tilde{p}})$ is a kernel function of feature vectors $\mathbf{d}_p$ and $\mathbf{d}_{\tilde{p}}$, which is utilized to map unseparate linearly feature samples from lower dimensional to higher dimensional, so that one can obtain the separable transformed features. There are several popular kernel function in practice and the Gaussian kernel function is employed in this paper, which is defined as

$$\kappa(\mathbf{d}_p, \mathbf{d}_{\tilde{p}}) = \exp(-\frac{\|\mathbf{d}_p - \mathbf{d}_{\tilde{p}}\|_2^2}{2\sigma^2}) \tag{24}$$

Aided by some famous convex optimization toolbox, convex quadratic programming problem (23) can be resolved efficiently, and the optimal solution is denoted as $\boldsymbol{\alpha}_l^\star = [\alpha_{l1}^\star, \ldots, \alpha_{lP}^\star]^\mathsf{T}$. Upon involving this optimal solution $\boldsymbol{\alpha}_l^\star$, the parameter $w_l^\star$ and $\varrho_l^\star$ can be represented by $\boldsymbol{\alpha}_l^\star$ as

$$\mathbf{w}_l^\star = \sum_{p=1}^{P} \alpha_{lp}^\star b_{lp} \phi(\mathbf{d}_p) \tag{25}$$

$$\begin{aligned} \varrho_l^\star &= \frac{1}{|\mathcal{V}|} \sum_{n\in\mathcal{V}} \left[b_{ln} - \mathbf{w}_l^{\star\mathsf{T}} \phi(\mathbf{d}_n) \right] \\ &= \frac{1}{|\mathcal{V}|} \sum_{n\in\mathcal{V}} \left[b_{ln} - \sum_{p=1}^{P} \alpha_{lp}^\star b_{lp} \phi(\mathbf{d}_p)^\mathsf{T} \phi(\mathbf{d}_n) \right] \\ &= \frac{1}{|\mathcal{V}|} \sum_{n\in\mathcal{V}} \left[b_{ln} - \sum_{p=1}^{P} \alpha_{lp}^\star b_{lp} \kappa(\mathbf{d}_p, \mathbf{d}_n) \right] \end{aligned} \tag{26}$$

where $\mathcal{V}$ is the index set of all support vectors and $|\mathcal{V}|$ denotes the cardinality of set $\mathcal{V}$.

- Step 9: Repeat step 8 for all $l \in \{1, \ldots, |\mathbb{L}|\}$

4) SIGNAL DETECTION

Once we get all $\boldsymbol{\alpha}_l^\star, l \in \{1, \ldots, |\mathbb{L}|\}$, a signal detection learning system may be built according to previous detailed steps. Hence, for any new coming bits group, it is manipulated into a real-valued feature vector and provided to the learning system. And consequently, the final result is the label of the prediction class, which corresponds the signal detection result. The detailed specific steps are as follows:

- Step 10: Input D received symbols as the test set data into the training model, and demodulate the obtained classification result into bit information for signal detection. Specifically, suppose all the classification results are stored in a D-dimensional row vector $\boldsymbol{\varsigma}$, we take the dth element $\varsigma_d, d = 1, \ldots, D$ of $\boldsymbol{\varsigma}$, and then subtract 1 from its value and convert it to binary, finally, the result is stored as the dth column in a matrix $\mathbf{X}$ with 4 rows and D columns.
- Step 11: Repeating step 10 until all D elements in $\boldsymbol{\varsigma}$ have been completed binary conversion.

D. THE PROPOSED SVM AIDED DETECTION ALGORITHM

By utilizing the classification idea and SVM approach, a signal detection algorithm is proposed with low complexity and good performance of the considered indoor GSM-VLC system. The algorithm is demonstrated in Algorithm 1.

Algorithm 1 : The Proposed SVM Aided Detection Algorithm

Training stage:
Input: received data sequence $\mathbf{y}$ for model training and testing;
1) denote the combination of the label set by $\mathbb{L}$, a collection of bit information as $\mathbb{I}$;
2) map received signal $\mathbf{y}$ to $\eta_{\text{GSM}}P$ bits stream to form $\mathbb{I}$, P data bits groups are obtained and each have η_{GSM} bits;
3) for the pth bits group $i_p \in \mathbb{I}$, one can obtain the corresponding label $l_p \in \mathbb{L}$, repeating this operation until the corresponding labels of all data bits groups $i_p, p = 1, \ldots, P$ are obtained, forming the label vector $\mathbf{b}$;
4) do one-vs-rest ($l -$ vs $- \bar{l}$) binary label classification;
for $l \in \{1, \ldots, |\mathbb{L}|\}$ **do**
  (23) - (26)
end
5) once we get all $\boldsymbol{\alpha}_l^\star$ for $l \in \{1, \ldots, |\mathbb{L}|\}$, a signal detection training system is built according to previous detailed steps.
Output: the trained detection model;
Detecting stage:
Input: received data sequence $\tilde{\mathbf{y}}$ for model testing or online detecting;
1) input received symbols $\tilde{\mathbf{y}}$ as the detection data into the trained model and obtain the classification label;
2) demodulate the obtained classification label into bit information for signal detection;
3) repeating until all received symbols have been completed binary conversion.
Output: the demodulated information bits;

IV. NUMERICAL AND SIMULATION RESULTS

This section will present the simulation results and performance analysis of the proposed SVM aided signal detection algorithm for the considered GSM-VLC system. In order to prove the performance of the proposed signal detection algorithm, we simulated an indoor environment with a size of $[5 \times 5 \times 3]$ m^3. We further assume that the emitting end LEDs are perpendicular to the ceiling and facing down to the floor, with a height of 3 m from the ground, the receiving end PDs are located away from the ceiling and on tables with a floor height of 0.85 m, it is also assumed that they are perpendicular to the table and face up to the ceiling. The half-power angle ($\Phi_{1/2}$) of the LED is set to 60°. The FoV half angle (Ψ_{FoV}) of the receiver PD is also set to 60°, and the size of the physical

TABLE 2. The spatial distribution coordinates of the LEDs' locations.

4 LEDs		8 LEDs	
LED	(O_X, O_Y, O_Z)	1	(1.25, 0.35 3) m
1	(1.25, 1.25, 3) m	2	(3.85, 0.35, 3) m
2	(3.25, 1.25, 3) m	3	(1.25, 1.85, 3) m
3	(1.25, 3.25, 3) m	4	(3.85, 1.85, 3) m
4	(3.25, 3.25, 3) m	5	(1.25, 3.25, 3) m
		6	(3.85, 3.25, 3) m
		7	(1.25, 4.25, 3) m
		8	(3.85, 4.25, 3) m

TABLE 3. System simulation parameters.

Room	Length (X)	5 m
	Width (Y)	5 m
	Height (Z)	3 m
Transmitter	No. of LEDs (N_t)	4, 8
	Height from floor	3 m
	LED semi-angle $(\Phi_{1/2})$	60°
	Modulation index (α)	0.1
	Average optical power per LED (P)	1 W
Receiver	No. of PDs (N_r)	4
	Height of table	0.85 m
	PD detection area (A_{PD})	1 cm^2
	FoV half angle of PD (Ψ_{FoV})	60°
	Optical filter gain T	1
	Refractive index (β)	1.5
	responsiveness of PD (R)	100 μA/mW

receiving area (A_{PD}) of each PD is 1 cm^2, the responsiveness of PD (R) is 100 μA/mW. The selection of LED position and simulation parameters are shown in Table 2 and Table 3.

A. BER PERFORMANCE ANALYSIS

In this section, we will present the BER performance simulation results of the proposed SVM aided signal detection algorithm in the considered GSM-VLC system, which is compared with some classical traditional signal detection algorithm, such as ML detection algorithm, KMC detection algorithm [15] and IKMC detection algorithm [16].

1) BER PERFORMANCE ANALYSIS OF SM-VLC SYSTEM

At first, we will demonstrate the BER performance simulation results of SM-VLC system with different detection algorithms, which are depicted in Fig. 4 and Fig. 5. In these simulations, it is assumed that the number of LEDs at the transmitting end is $N_t = 4$ or 8, the number of PDs at the receiving end is $N_r = 4$, the number of activated LEDs in each time slot is $n_t = 1$ and the number of symbols is $M = 2$.

From Fig. 4 and Fig. 5, we can obtain that the traditional KMC detection algorithm has an error platform effect when the signal-to-noise ratio (SNR) is high, although this problem can be alleviated by increasing the number of algorithm operation, but it still can't be completely resolved. Although the IKMC detection algorithm can solve the error platform problem, however, as can be seen from Fig. 4 and Fig. 5 that there is still an obvious BER performance gap between the IKMC detection algorithm and the SVM-based detection algorithm and the ML detection algorithm. In addition, the BER performance of our proposed SVM aided signal detection algorithm

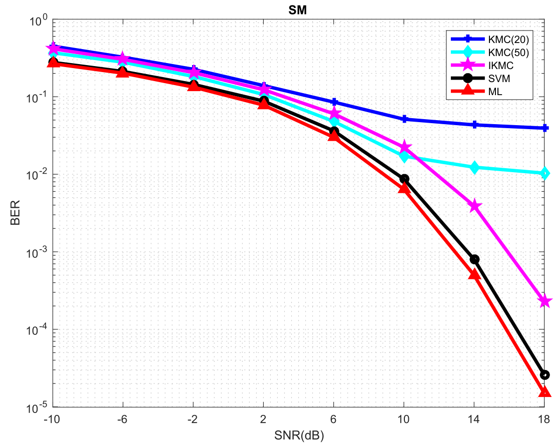

FIGURE 4. BER performance analysis of KMC detector, IKMC detector, proposed SVM aided detector and ML detector of SM-VLC system with system configuration: $N_t = 4, N_r = 4, n_t = 1, M = 2$.

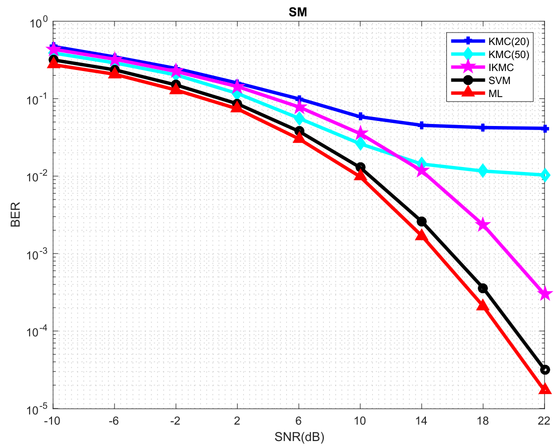

FIGURE 5. BER performance analysis of KMC detector, IKMC detector, proposed SVM aided detector and ML detector of SM-VLC system with system configuration: $N_t = 8, N_r = 4, n_t = 1, M = 2$.

is better than traditional KMC detection and IKMC detection, and is close to ML detection algorithm. For example, the performance difference between our proposed SVM aided signal detection algorithm and ML detection algorithm is less than 0.7 dB when BER is 10^{-4}.

2) BER PERFORMANCE ANALYSIS OF GSM-VLC SYSTEM

Then, the BER performance simulation results of GSM-VLC system with different detection algorithms are demonstrated in this simulation, which are depicted in Fig. 6 and Fig. 7. In this simulation, we assume that the number of LEDs at the transmitting end is $N_t = 4$ or 8, the number of PDs at the receiving end is $N_r = 4$, the number of activated LEDs in each time slot is $n_t = 2$ and the number of symbols is $M = 2$.

From Fig. 6 and Fig. 7, we can learn that the traditional KMC detector still has a serious error platform effect when the SNR is higher than 10 dB. Although the IKMC detection algorithm can solve the error platform problem of KMC

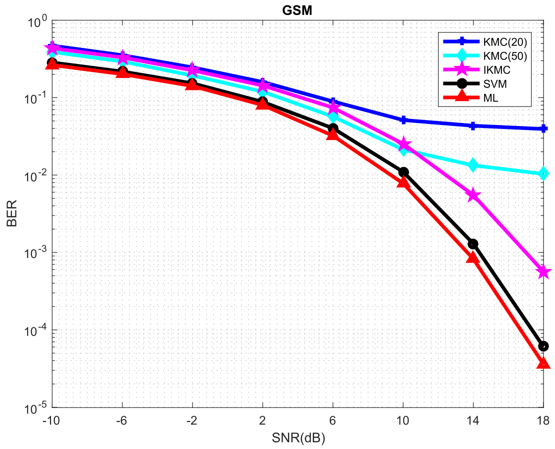

FIGURE 6. BER performance analysis of KMC detector, IKMC detector, proposed SVM aided detector and ML detector of GSM-VLC system with system configuration: $N_t = 4, N_r = 4, n_t = 2, M = 2$.

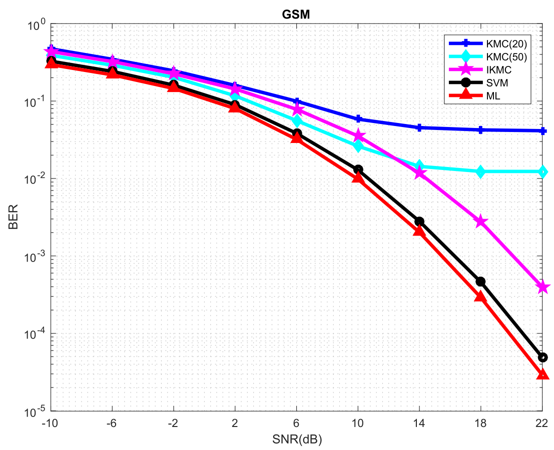

FIGURE 7. BER performance analysis of KMC detector, IKMC detector, proposed SVM aided detector and ML detector of GSM-VLC system with system configuration: $N_t = 8, N_r = 4, n_t = 2, M = 2$.

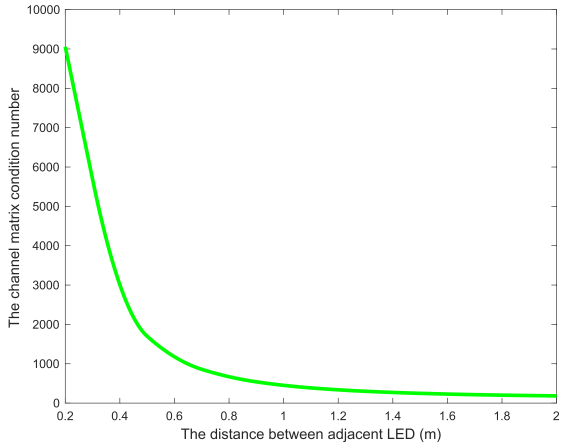

FIGURE 8. The relationship between channel matrix condition number and the LEDs spacing.

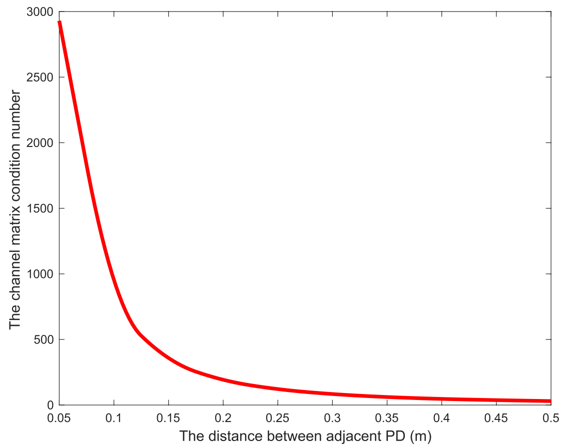

FIGURE 9. The relationship between channel matrix condition number and the PDs spacing.

detector, however, as can be seen from Fig. 6 and Fig. 7 that there is still about 5 dB BER performance gap between the IKMC detection algorithm and the SVM based detection algorithm and the ML detector. In addition, the BER performance of our proposed SVM aided signal detection algorithm outperforms both the traditional KMC and the IKMC detector, which has approached to ML detection algorithm. When the BER is 10^{-4}, the performance difference between SVM aided signal detection algorithm and ML detection algorithm is less than 0.6 dB. The simulation analysis further verifies the effectiveness of the proposed SVM aided signal detection algorithm.

Comparing the simulation results of SM-VLC and GSM-VLC two different situations with four various detection algorithms in Fig. 4 - Fig. 7, it can be concluded that the BER performance of the proposed signal detection algorithm aided by SVM is close to the optimal ML detector, and obviously superior than KMC and IKMC detectors, especially in relatively high SNR region.

B. CORRELATION ANALYSIS

Based on the results obtained in [25], the channel spatial correlation of indoor GSM-VLC system is mainly affected by the spatial locations' distribution of LEDs and PDs. For a typical application scenario with indoor GSM-VLC system, we assume that the number of LEDs and PDs are both 4, and by utilizing channel matrix condition number as the measure of spatial correlation of MIMO channel, the condition number of channel matrix versus the distance between each LED is demonstrated in Fig. 8, where the vertical distance between LEDs and PDs is set as 2.15 m. And similarly, the condition number of channel matrix versus the distance between each PD is demonstrated in Fig. 9, where the vertical distance between LED and PD is also set as 2.15 m. Furthermore, the condition number of channel matrix versus the vertical distance between LEDs and PDs is depicted in Fig. 10, where the distance between adjacent LEDs is set as 2 m and adjacent PDs is set as 0.2 m, respectively. From Fig. 8 to Fig. 10, we can learn that the channel spatial correlation becomes stronger with the decreasing of LEDs spacing, PDs spacing,

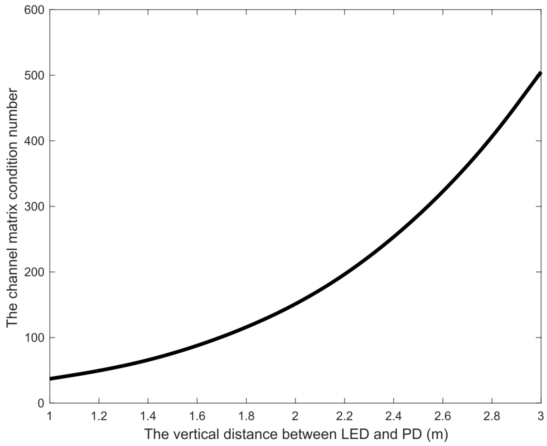

FIGURE 10. The relationship between channel matrix condition number and the vertical distance of LED and PD.

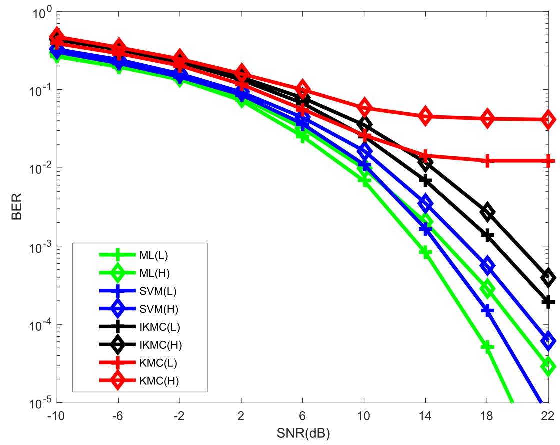

FIGURE 11. BER performance analysis of KMC detector, IKMC detector, proposed SVM aided detector and ML detector of GSM-VLC system with different LEDs distances.

TABLE 4. The spatial distributions of LEDs' locations with $N_t = 4, 8$.

4 LEDs		8 LEDs	
LED	(O_X, O_Y, O_Z)	1	(2.25, 0.85 3) m
1	(1.25, 1.25, 3) m	2	(3.25, 0.85, 3) m
2	(3.25, 1.25, 3) m	3	(2.25, 1.85, 3) m
3	(1.25, 3.25, 3) m	4	(3.25, 1.85, 3) m
4	(3.25, 3.25, 3) m	5	(2.25, 2.85, 3) m
		6	(3.25, 2.85, 3) m
		7	(2.25, 3.85, 3) m
		8	(3.25, 3.85, 3) m

TABLE 5. The spatial distributions of PDs' locations with $N_r = 4, 8$.

4 PDs		8 PDs	
PD	(O_X, O_Y, O_Z)	1	(2.5, 2.4, 0.8) m
1	(2.3, 2.3, 0.8) m	2	(2.5, 2.5, 0.8) m
2	(2.3, 2.7, 0.8) m	3	(2.5, 2.6, 0.8) m
3	(2.7, 2.3, 0.8) m	4	(2.5, 2.7, 0.8) m
4	(2.7, 2.7, 0.8) m	5	(2.6, 2.4, 0.8) m
		6	(2.6, 2.5, 0.8) m
		7	(2.6, 2.6, 0.8) m
		8	(2.6, 2.7, 0.8) m

and the increasing of the vertical distance between LEDs and PDs.

Next, in order to test the influence of spatial correlation of MIMO channel in our considered GSM-VLC system on the proposed SVD aided detection approach and other detectors, the following simulation are designed.

At first, the simulations are designed to test the impact of changing the LEDs spacing on the detection performance of different detectors, while all other parameters are fixed. Specifically, assuming that the number of LEDs and PDs are $N_t = 4, 8$ and $N_r = 4$, respectively. We assume the number of activated LEDs in each time slot is $n_t = 2$, and the order of the IM PAM is $|M| = 2$. We also assume that the distance between adjacent PDs is fixed at 0.2 m, the vertical distance from LEDs to PDs is fixed as 2.15 m, and furthermore the locations of LEDs are provided in Table 4. It can be seen from Table 4 that when the number of LEDs changes from 4 to 8, the distance between adjacent LEDs becomes smaller. From the previous analysis results, when the distance between adjacent LEDs decreases, the channel spatial correlation becomes stronger. The simulation results are shown in Fig. 11. Note that in Fig. 11, the symbol '(H)' represents the results of $N_t = 8$, while '(L)' represents the results of $N_t = 4$, respectively. It can be seen from Fig. 11 that when the LEDs spacing becomes smaller, the detection performance of all the detectors becomes worse. Although the performance of all detection algorithms has been reduced, the detection performance of the proposed SVM based detection algorithm is still close to the optimal ML detector.

Then, the simulations are designed to verify the impact of changing the PDs spacing on the detection performance of different detectors, while all other parameters are fixed. Specifically, we assume that the number of LEDs and PDs are $N_t = 8$ and $N_r = 4, 8$, the number of activated LEDs in each time slot is $n_t = 2$, and the order of the IM PAM is $|M| = 2$. We also assume that the distance between adjacent LEDs is fixed at 1 m, the vertical distance from LEDs to PDs is fixed at 2.15 m, and furthermore the locations of PDs are provided in Table 5. From Table 5 we learn that when the number of PDs is 4, the distance between adjacent PDs is 0.4 m, while when the number of PDs is 8, the distance between adjacent PDs is 0.1 m. Again, from the previous analysis results, when the distance between adjacent PDs decreases, the channel spatial correlation becomes stronger. The simulation results are shown in Fig. 11, where the symbol '(H)' represents the results of $N_r = 8$, while '(L)' represents the results of $N_r = 4$, respectively. Observe from the simulation results that when the LEDs spacing becomes smaller, again the detection performance of all the detectors becomes worse. Although the performance of all detection algorithms is reduced when the channel spatial correlation becomes stronger, the detection performance of the proposed SVM based detection algorithm is still close to the optimal ML detector.

Finally, the simulations are designed to examine the impact of changing the vertical distance between LEDs and PDs

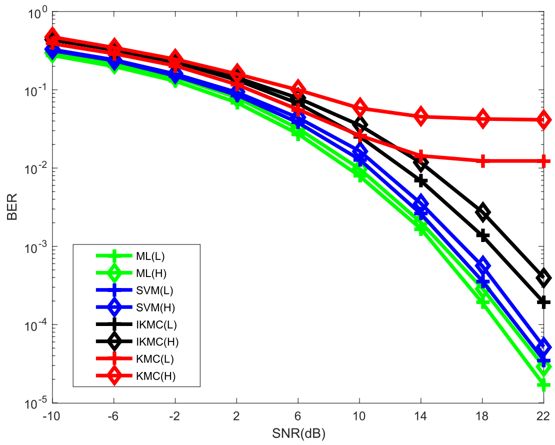

FIGURE 12. BER performance analysis of KMC detector, IKMC detector, proposed SVM aided detector and ML detector of GSM-VLC system with different PDs distances.

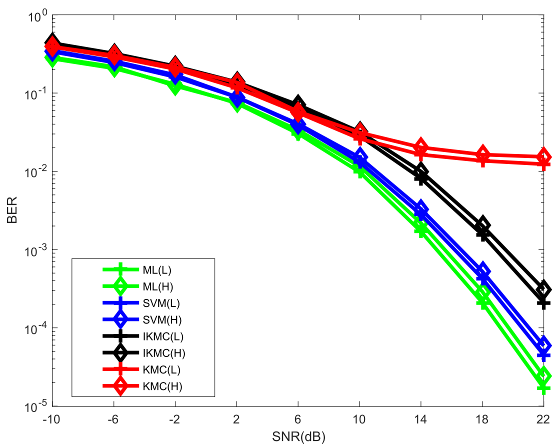

FIGURE 13. BER performance analysis of KMC detector, IKMC detector, proposed SVM aided detector and ML detector of GSM-VLC system with different vertical distances between LEDs and PDs: 2 m and 1 m.

on the performance of different detection algorithms, while all other parameters are fixed. Specifically, we assume that the number of LEDs and PDs are $N_t = 8$ and $N_r = 4$, respectively. The number of activated LEDs in each time slot is $n_t = 2$, and the order of the IM PAM is $|M| = 2$. We further assume that the locations of LEDs are the same as in Table 2 with $N_t = 8$ and the distance between adjacent PDs are set as 0.2 m, the vertical distance between LEDs and PDs are set as two cases: 2 m and 1 m. The simulation results are demonstrated in Fig. 13, where the symbol '(H)' represents a vertical distance of 2 m, while '(L)' represents a vertical distance of 1 m.

It can be observed from Fig. 13 that when the vertical distance between LEDs and PDs is reduced, the detection performance of all the detectors becomes better. Additionally, we can also learn that when the vertical distance between LEDs and PDs is changed, the performance of all detectors does not change significantly, this is due to change the vertical distance has limited impact on the channel spatial correlation, as the simulation results provided in Fig. 13.

TABLE 6. Complexity orders of various detectors for the indoor GSM-VLC system.

Detection algorithm	Complexity order
KMC	$\mathcal{O}(FL\eta_{\text{GSM}}n_{\text{iter}})$
IKMC	$\mathcal{O}(L^2 + L\eta_{\text{GSM}}n_{\text{iter}})$
ML	$\mathcal{O}(LN_rN_t2^{\eta_{\text{GSM}}})$
SVM	$\mathcal{O}(L\eta_{\text{GSM}})$

Consequently, we can conclude that, with stronger channel spatial correlation, the worse detection performance will be obtained by the proposed SVM aided detector and the other detection algorithms of our considered GSM-VLC system. Among three factors of the LEDs spacing, the PDs spacing and the vertical distance between LEDs and PDs, the vertical distance between LEDs and PDs has the least effect on the performance of the detection algorithm, then is the PDs spacing, while the LEDs spacing has the greatest impact on detection performance.

Therefore, for actual indoor VLC application scenarios, because the distribution space region of PDs is limited and the vertical distance between LEDs and PDs are also determined in advance, the channel spatial correlation is mainly determined by LEDs spacing. When the number of LEDs at the transmitting end increases, the LEDs spacing will be reduced, and eventually the channel spatial correlation becomes stronger, and the detection performance of the proposed SVM aided detector and other detectors will be deteriorated unavoidably. Consequently, we should try to layout the locations distribution of LEDs to make the adjacent spacing as large as possible.

C. COMPLEXITY ANALYSIS

The previous simulation experiments have verified the BER performance of the proposed SVM aided signal detection algorithm in the indoor GSM-VLC system considered in this paper, and the results show that it is close to the optimal ML detection algorithm. Following this, the superiority of the algorithm proposed in this paper will be verified from the computational complexity aspect.

Aided by the complexity analysis of the conventional KMC and IKMC detector in [15], [16], in this paper, the complexities of the proposed and other detectors are compared in Table 6, where L is the length of transmit signal sequence, F is the number of loop in KMC algorithm and n_{iter} is the number of iterations of the KMC and IKMC detection algorithms in each loop. It should be noted that, in general case, L is set as tens or hundreds, and when there are more LEDs and higher modulation order $|M|$, the value of F needs to be hundreds or even thousands to obtain the convergence of algorithm KMC, which makes the complexity of both KMC and IKMC detectors very large. It can be seen from Table 6 that the computational complexity of the SVM aided signal detection algorithm proposed in this paper is significantly lower than that of the traditional signal detection algorithm.

Through the comprehensive consideration of BER performance analysis and computational complexity analysis of various algorithms, the SVM aided signal detection algorithm proposed in this paper has appropriate comprehensive performance in the considered indoor GSM-VLC system, which effectively improves the system efficiency.

V. CONCLUSION

Aiming at the channel characteristics of indoor GSM-VLC system, this paper models the signal detection problem of indoor GSM-VLC system as a multiple classification problem, and proposes a low-complexity and high-efficiency signal detection algorithm based on SVM. By randomly generated independent and identically distributed symbol data, a training sample set was obtained and a label vector of the this training sample set was then constructed. Following this, the kernel SVM was utilized to formulate the optimization problem of signal detection. Aided by the dual theory, the dual problem of the quadratic convex programming of the original problem was formulated to efficiently obtain the optimal classification parameters of the SVM. Finally, the online signal detection of any given received symbol data was realized by taking advantage of the optimal classification parameters obtained by the proposed learning scheme. Compared with traditional signal detection algorithms, the algorithm proposed in this paper can achieve BER performance close to the optimal detector with considerable lower computational complexity.

REFERENCES

[1] H. Elgala, R. Mesleh, and H. Haas, ''Indoor optical wireless communication: Potential and state-of-the-art,'' *IEEE Commun. Mag.*, vol. 49, no. 9, pp. 56–62, Sep. 2011.

[2] D. Karunatilaka, F. Zafar, V. Kalavally, and R. Parthiban, ''LED based indoor visible light communications: State of the art,'' *IEEE Commun. Surveys Tuts.*, vol. 17, no. 3, pp. 1649–1678, 3rd Quart., 2015.

[3] S. Wu, H. Wang, and C.-H. Youn, ''Visible light communications for 5G wireless networking systems: From fixed to mobile communications,'' *IEEE Netw.*, vol. 28, no. 6, pp. 41–45, Nov. 2014.

[4] F. Wang, C. Liu, Q. Wang, J. Zhang, R. Zhang, L.-L. Yang, and L. Hanzo, ''Optical jamming enhances the secrecy performance of the generalized space-shift-keying-aided visible-light downlink,'' *IEEE Trans. Commun.*, vol. 66, no. 9, pp. 4087–4102, Sep. 2018.

[5] P. Liu, J. Blumenstein, N. S. Perovic, M. Di Renzo, and A. Springer, ''Performance of generalized spatial modulation MIMO over measured 60 GHz indoor channels,'' *IEEE Trans. Commun.*, vol. 66, no. 1, pp. 133–148, Jan. 2018.

[6] W. Liu, Y. Zhang, and M. Jin, ''Lagrangian detection for generalized space-shift keying MIMO systems,'' *IEEE Trans. Veh. Technol.*, vol. 66, no. 9, pp. 8585–8589, Sep. 2017.

[7] X. Zhang, Q. Liu, and M. Jin, ''Detection of generalized space shift keying signal with sparse reconstruction,'' *IEEE Trans. Veh. Technol.*, vol. 66, no. 6, pp. 5471–5475, Jun. 2017.

[8] J. Jeganathan, A. Ghrayeb, and L. Szczecinski, ''Generalized space shift keying modulation for MIMO channels,'' in *Proc. IEEE 19th Int. Symp. Pers., Indoor Mobile Radio Commun.*, Sep. 2008, pp. 1–5.

[9] H. Li, F. Wang, J. Zhang, and C. Liu, ''Secrecy performance analysis of MISO visible light communication systems with spatial modulation,'' *Digit. Signal Process.*, vol. 81, pp. 116–128, Oct. 2018.

[10] F. Wang, R. Li, J. Zhang, S. Shi, and C. Liu, ''Enhancing the secrecy performance of the spatial modulation aided VLC systems with optical jamming,'' *Signal Process.*, vol. 157, pp. 288–302, Apr. 2019.

[11] T. Fath and H. Haas, ''Performance comparison of MIMO techniques for optical wireless communications in indoor environments,'' *IEEE Trans. Commun.*, vol. 61, no. 2, pp. 733–742, Feb. 2013.

[12] T. Q. Wang, Y. A. Sekercioglu, and J. Armstrong, ''Analysis of an optical wireless receiver using a hemispherical lens with application in MIMO visible light communications,'' *J. Lightw. Technol.*, vol. 31, no. 11, pp. 1744–1754, Jun. 2013.

[13] K. Ying, H. Qian, R. J. Baxley, and S. Yao, ''Joint optimization of precoder and equalizer in MIMO VLC systems,'' *IEEE J. Sel. Areas Commun.*, vol. 33, no. 9, pp. 1949–1958, Sep. 2015.

[14] S. Ruping and K. Morik, ''Support vector machines and learning about time,'' in *Proc. IEEE Int. Conf. Acoust., Speech, Signal Process. (ICASSP)*, vol. 4, Apr. 2003, pp. 4–864.

[15] H.-W. Liang, W.-H. Chung, and S.-Y. Kuo, ''Coding-aided K-means clustering blind transceiver for space shift keying MIMO systems,'' *IEEE Trans. Wireless Commun.*, vol. 15, no. 1, pp. 103–115, Jan. 2016.

[16] L. You, P. Yang, Y. Xiao, S. Rong, D. Ke, and S. Li, ''Blind detection for spatial modulation systems based on clustering,'' *IEEE Commun. Lett.*, vol. 21, no. 11, pp. 2392–2395, Nov. 2017.

[17] L. Zhang and M. Jin, ''A constrained clustering-based blind detector for spatial modulation,'' *IEEE Commun. Lett.*, vol. 23, no. 7, pp. 1170–1173, Jul. 2019.

[18] R. Jiang, C. Sun, L. Zhang, X. Tang, H. Wang, and A. Zhang, ''Deep learning aided signal detection for SPAD-based underwater optical wireless communications,'' *IEEE Access*, vol. 8, pp. 20363–20374, 2020.

[19] H. Lee, I. Lee, and S. H. Lee, ''Deep learning based transceiver design for multi-colored VLC systems,'' *Opt. Exp.*, vol. 26, no. 5, p. 6222, 2018.

[20] Y. Yuan, M. Zhang, P. Luo, Z. Ghassemlooy, L. Lang, D. Wang, B. Zhang, and D. Han, ''SVM-based detection in visible light communications,'' *Optik*, vol. 151, pp. 55–64, Dec. 2017.

[21] A. Mostafa and L. Lampe, ''Physical-layer security for MISO visible light communication channels,'' *IEEE J. Sel. Areas Commun.*, vol. 33, no. 9, pp. 1806–1818, Sep. 2015.

[22] A. Mostafa and L. Lampe, ''Optimal and robust beamforming for secure transmission in MISO visible-light communication links,'' *IEEE Trans. Signal Process.*, vol. 64, no. 24, pp. 6501–6516, Dec. 2016.

[23] T. Komine and M. Nakagawa, ''Fundamental analysis for visible-light communication system using LED lights,'' *IEEE Trans. Consum. Electron.*, vol. 50, no. 1, pp. 100–107, Feb. 2004.

[24] T. Handte, A. Müller, and J. Speidel, ''BER analysis and optimization of generalized spatial modulation in correlated fading channels,'' in *Proc. IEEE 70th Veh. Technol. Conf. Fall*, Sep. 2009, pp. 1–5.

[25] S. Xiao, K. Huang, Z. Zhong, and X. Jin, ''Spatial correlation analysis of MIMO channel in indoor visible light communication,'' *J. Electron. Inf. Technol.*, vol. 36, no. 9, pp. 2117–2123, 2014.

HAOBO SUN is currently pursuing the master's degree with the School of Information Engineering, Zhengzhou University, China. His research interests include visible light communication and machine learning.

YANBIN ZHANG received the Ph.D. degree in information and communication engineering from the Beijing Institute of Technology, China, in 2009. He is currently a Lecturer with the School of Information Engineering, Zhengzhou University, China. His current research interests include real time signal processing, wireless communications, and embedded systems.

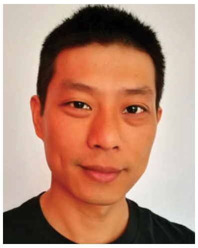

FASONG WANG received the B.Sc. and M.Sc. degrees in applied mathematics from the China University of Geosciences, China, in 2002 and 2005, respectively, and the Ph.D. degree in communication engineering from Xidian University, in 2013. He worked as a Senior Engineer with the China Electronics Technology Group Corporation, the 27th Research Institute, Zhengzhou, Henan, China, in 2010. From 2016 to 2017, he was a Visiting Scholar with the Southampton Wireless Group, University of Southampton. He is currently a Professor with the School of Information Engineering, Zhengzhou University, China. His current research interests include visible light communication, blind signal processing, sparse representation, machine learning, and their applications. He has published more than 40 journal articles and conference papers on these topics.

JIANKANG ZHANG (Senior Member, IEEE) received the B.Sc. degree in mathematics and applied mathematics from the Beijing University of Posts and Telecommunications, in 2006, and the Ph.D. degree in communication and information systems from Zhengzhou University, in 2012. He was a Senior Research Fellow with the University of Southampton, U.K. From 2012 to 2013, he was a Lecturer with Zhengzhou University, where he was an Associate Professor, from 2013 to 2014. From 2009 to 2011, he was a Visiting Ph.D. Student with the School of Electronics and Computer Science, University of Southampton. From 2013 to 2014, he was a Postdoctoral Researcher with McGill University, Canada. He is currently a Senior Lecturer with Bournemouth University. His research interests include aeronautical communications, aeronautical networks, and evolutionary algorithms. He was a recipient of a number of academic awards, including the Excellent Doctoral Dissertation of Henan Province, China, the Youth Science and Technology Award of Henan Province, China, and the Innovative Talent of Colleges and Universities of Henan Province, China. He serves as an Associate Editor for IEEE ACCESS.

SHIJIE SHI received the B.Eng. degree in information engineering and the Ph.D. degree in communication and information systems from the China University of Mining and Technology, Xuzhou, China, in 2009 and 2016, respectively. From 2013 to 2014, he was a Ph.D. Student with the ICT, CSIRO, Sydney, NSW, Australia. Since 2016, he has been with the College of Information Engineering, Zhengzhou University, where he is currently a Lecturer. His current research interests include resource allocation and access control in vehicular networks, cooperative relay networks, and self-organizing networks.